THE JOURNAL OF PHYSICAL CHEMISTRY Letters

Letter

pubs.acs.org/JPCL

Electron Spin Manipulation via Encaged Cluster: Differing Anion Radicals of $Y_2@C_{82}$-C_s, $Y_2C_2@C_{82}$-C_s, and $Sc_2C_2@C_{82}$-C_s

Yihan Ma,[†] Taishan Wang,*[,†] Jingyi Wu,[‡] Yongqiang Feng,[†] Hui Li,[†] Li Jiang,[†] Chunying Shu,[†] and Chunru Wang*[,†]

[†]Beijing National Laboratory for Molecular Sciences, Laboratory of Molecular Nanostructure and Nanotechnology, Institute of Chemistry, Beijing 100190, China

[‡]Laboratory of Nuclear Analysis Techniques, Institute of High Energy Physics, Chinese Academy of Sciences, Beijing, 100049, China

Supporting Information

ABSTRACT: Endohedral metallofullerene species with controllable electron spin have attracted increasing attention along with their potential application in quantum information processing. In this paper, we report the electron spin manipulation via encage cluster through comparative studies on the anion radicals of metallofullerene $Y_2@C_{82}$-C_s, $Y_2C_2@C_{82}$-C_s, and $Sc_2C_2@C_{82}$-C_s. Although these three radical species have the same parent fullerene cage, we found that the unpaired spin characteristics as well as metal-spin couplings of them can be greatly affected by endohedral clusters. Furthermore, based on theoretical calculations, it was revealed that the encaged clusters can affect the electronic population of pristine endohedral metallofullerenes and eventually manipulate the spin distribution of their corresponding anion radicals. Our findings are referential to the spin coherence in information processing due to the variable paramagnetism of these metallofullerene radicals.

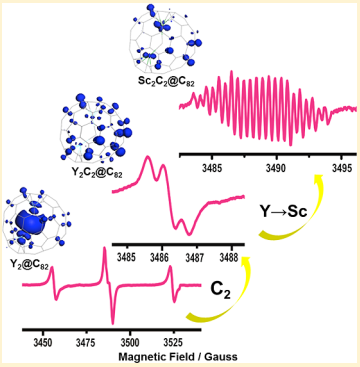

SECTION: Molecular Structure, Quantum Chemistry, and General Theory

Endohedral metallofullerenes are constructed by fullerene cages encapsulating metal ions or clusters, and their unique structures have brought many novel physical and chemical properties.[1−4] For example, some endohedral metallofullerene radicals, e.g., $Sc@C_{82}$, $Y@C_{82}$, $Sc_3C_2@C_{80}$ etc., show extremely high stability due to the delocalized or even embedded unpaired spin by the fullerene cages.[5−7] Recently, along with the rapid progresses on quantum information processing and quantum computing, the manipulation of electron spin has become a hot subject;[8−10] thus, endohedral metallofullerene radicals with stable and controllable electron spins will have important application prospects.

In general, the manipulation of electron spin on a paramagnetic metallofullerene involves the electron spin distribution on fullerene molecules, the interaction between the fullerene cage and internal species, the couplings between the metal nuclei and unpaired spin, and the thermal rotation of the internal species, etc.[11,12] In order to explore how the electron spin distributions were manipulated by the endohedral species, here three endohedral metallofullerenes $Y_2@C_{82}$-C_s, $Y_2C_2@C_{82}$-C_s, and $Sc_2C_2@C_{82}$-C_s with the same parent fullerene cage were chosen, and a comparison study on their radical properties was performed.

$Y_2@C_{82}$-C_s, $Y_2C_2@C_{82}$-C_s, and $Sc_2C_2@C_{82}$-C_s samples were prepared by the Krätschmer−Huffman arc discharging method and isolated by high-performance liquid chromatography (HPLC). The purity of the three samples was confirmed by both the HPLC analysis and matrix-assisted laser desorption ionization time-of-flight (MALDI-TOF) mass spectrometry (see Supporting Information (SI)). Since the structures of $Y_2@C_{82}$-C_s, $Y_2C_2@C_{82}$-C_s, and $Sc_2C_2@C_{82}$-C_s molecules have been characterized by single crystal X-ray analysis and NMR method in literature,[13−15] here only comparative Raman and ultraviolet/visible−near infrared (UV/vis−NIR) absorption spectroscopic studies on them were performed (see SI). It was revealed that the UV/vis-NIR absorption spectra of $Y_2@C_{82}$, $Y_2C_2@C_{82}$, and $Sc_2C_2@C_{82}$ resemble each other, and show similar spectral features with the related literature.[13−15] As for Raman spectroscopy, the three molecules exhibit analogous spectral features in the region between 1000 and 1600 cm^{-1}, corresponding to the C_{82}-C_s cage tangential vibrations, and quite large difference in the region between 100 and 600 cm^{-1}, corresponding to the vibrations from different encaged clusters.

The anion radicals of $Y_2@C_{82}$-C_s, $Y_2C_2@C_{82}$-C_s, and $Sc_2C_2@C_{82}$-C_s were prepared by contacting potassium metal with the samples in tetrahydrofuran (THF) solution several times under nitrogen atmosphere. Then the resulting anion radicals were measured by electron spin resonance (ESR) spectroscopy with continuous Xband wave at room temperature.

The ESR spectra of the $Y_2@C_{82}$-C_s, $Y_2C_2@C_{82}$-C_s, and $Sc_2C_2@C_{82}$-C_s anion radicals were successfully obtained shown in Figure 1. For $Y_2@C_{82}$-C_s anion radical, the ESR spectrum

Received: December 12, 2012
Accepted: January 15, 2013

   dx.doi.org/10.1021/jz3020666 | J. Phys. Chem. Lett. 2013, 4, 464−467

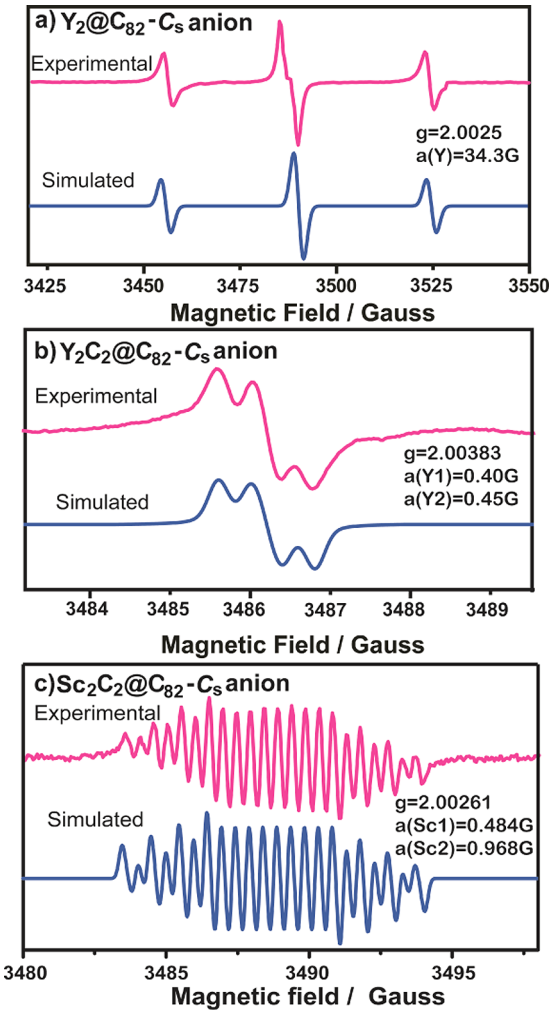

Figure 1. The experimental and simulated ESR spectra of $Y_2@C_{82}$-C_s (a), $Y_2C_2@C_{82}$-C_s (b), and $Sc_2C_2@C_{82}$-C_s (c) anion radicals.

displays three groups of signals with a 1:2:1 intensity ratio due to the couplings between the unpaired spin and the two equivalent ^{89}Y nuclei (I = 1/2), and the hyperfine coupling constant (hfcc) was identified at 34.3 G (2 nuclei) and the g value of 2.0025. On the contrary, the ESR spectra of both $Y_2C_2@C_{82}$-C_s and $Sc_2C_2@C_{82}$-C_s show unsymmetrical features, and the hfcc and g values are a(Y1) = 0.4 G, a(Y2) = 0.45 G, g = 2.00383 for $Y_2C_2@C_{82}$-C_s, and a(Sc1) = 0.484 G, a(Sc2) = 0.968 G, g = 2.00261 for $Sc_2C_2@C_{82}$-C_s, respectively.

In ESR studying, the large hfcc usually means the unpaired spin is mainly localized on the metal nuclei, so the larger hfcc of $Y_2@C_{82}$-C_s anion radical indicates that the unpaired spin is located on the two yttrium nuclei. Similar behaviors have been reported for $Sc_3N@C_{80}$ anion radical with hfcc at 55.7 G,[16] $Y_2@C_{79}N$ molecule with hfcc at 81.23 G,[17] and $Sc_4O_2@C_{80}$ cation radical with hfcc at 150.4 G.[18] However, both $Y_2C_2@C_{82}$-C_s and $Sc_2C_2@C_{82}$-C_s anion radicals have comparatively tiny hfcc values (<1 G), suggesting that the unpaired spin must not localize on the endohedral clusters but mainly on the C_{82} cage as discussed below.

The spin density distributions of $Y_2@C_{82}$-C_s, $Y_2C_2@C_{82}$-C_s, and $Sc_2C_2@C_{82}$-C_s anion radicals were studied through theoretical calculations.[19,20] As shown in Figure 2, it was revealed that the unpaired spin is mainly localized on the two yttrium nuclei for $Y_2@C_{82}$-C_s anion radical, which is highly

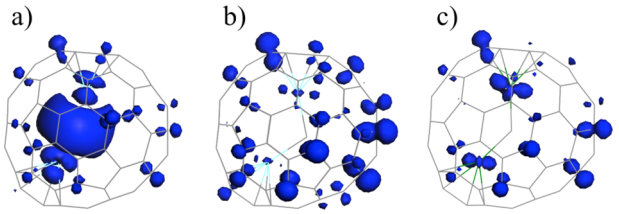

Figure 2. The calculated spin density distributions of $Y_2@C_{82}$-C_s (a), $Y_2C_2@C_{82}$-C_s (b), and $Sc_2C_2@C_{82}$-C_s (c) anion radicals. The blue area presents the unpaired spin.

consistent with experimental result. Surprisingly, after introducing the C_2 into the C_{82}-C_s fullerene cage, both $Y_2C_2@C_{82}$-C_s and $Sc_2C_2@C_{82}$-C_s anion radicals have their unpaired spin predominantly localizing on the carbon cage. However, comparing to $Y_2C_2@C_{82}$-C_s radical, the $Sc_2C_2@C_{82}$-C_s anion radical has more spin distributions on the encaged metal ions. On the basis of the above studies, therefore, the electron spin of the C_{82}-C_s-based metallofullerenes can be manipulated by introducing the C_2 into the endohedral moiety, and further fine manipulation of the spin distributions on metallofullerenes can be achieved by changing the metal ions, e.g., from yttrium to scandium.

To deepen our understanding about the spin manipulations, frontier molecular orbitals of $Y_2@C_{82}$-C_s, $Y_2C_2@C_{82}$-C_s, and $Sc_2C_2@C_{82}$-C_s were analyzed, as shown in Figure 3. It was

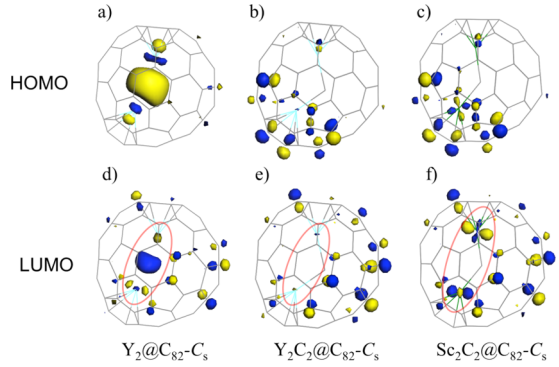

Figure 3. Molecular orbitals of pristine $Y_2@C_{82}$-C_s, $Y_2C_2@C_{82}$-C_s, and $Sc_2C_2@C_{82}$-C_s. The LUMOs locate on the three endohedral clusters are denoted by red circles, respectively.

revealed that the lowest unoccupied molecular orbitals (LUMOs) of $Y_2@C_{82}$-C_s mainly localize on the Y−Y bonding, while those of $Y_2C_2@C_{82}$-C_s mainly localize on the carbon cage, so it is naturally accountable to observe the large differences in their spin distributions while an extra electron is added to the two metallofullerenes. As a comparison, although the LUMOs of $Sc_2C_2@C_{82}$-C_s mainly localize on the fullerene cage, a minor contribution is also observed from the two scandium atoms, so relatively larger hfcc values are expected for $Sc_2C_2@C_{82}$-C_s comparing with $Y_2C_2@C_{82}$-C_s.

The differences on the frontier orbitals of $Y_2@C_{82}$-C_s, $Y_2C_2@C_{82}$-C_s, and $Sc_2C_2@C_{82}$-C_s also can be reflected via their reactivity. The Bingel−Hirsch reaction[21] on above-mentioned metallofullerenes was tested, since this reaction was known as a typical nucleophilic addition process for metallofullerenes, and the population of LUMOs on fullerene cages would influence such reactivity. Since the resulting carbanions would easily attack the cage-dominated LUMOs, it is expected that $Y_2C_2@$

dx.doi.org/10.1021/jz3020666 | J. Phys. Chem. Lett. 2013, 4, 464−467

C_{82}-C_s is easy to execute the Bingel–Hirsch reaction, Sc_2C_2@C_{82}-C_s the next, and Y_2@C_{82}-C_s may be difficult to react because of its poor LUMO distributions on the fullerene cage.

The Bingel–Hirsch reaction products were checked by HPLC, where the relevant ratios of the products to reactants can be directly imaged by combining with MALDI-TOF analysis of the composition of each fraction (see SI). As shown in Figure 4, Y_2C_2@C_{82}-C_s was indeed very easy to react, in

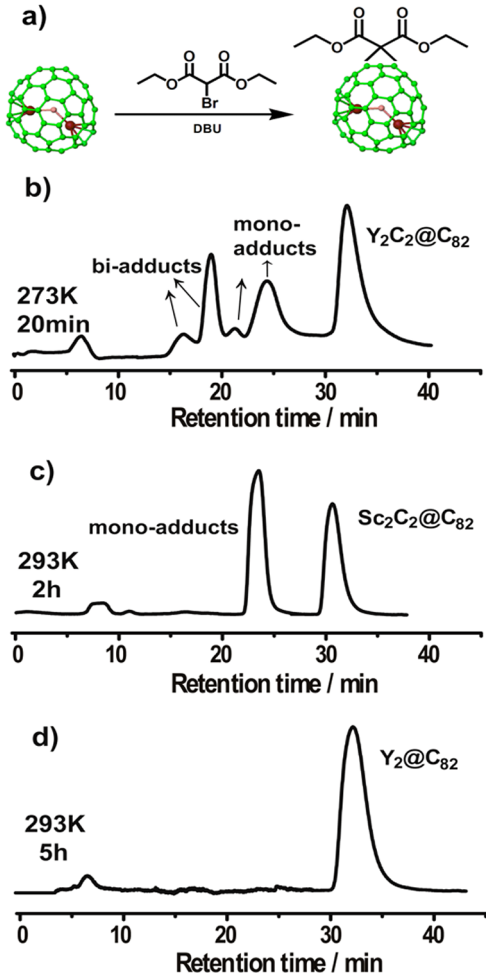

Figure 4. The Bingel–Hirsch reaction (a) and HPLC profiles of the reaction products of Y_2C_2@C_{82}-C_s (b), Sc_2C_2@C_{82}-C_s (c), and Y_2@C_{82}-C_s (d). The reaction temperature and time are shown on the each HPLC profile respectively.

which abundant derivatives were observed after only 20 min at 273 K, and for Sc_2C_2@C_{82}-C_s, its monoadducts were observed after 2 h at 293 K. However, Y_2@C_{82}-C_s did not react at all, even after 5 h at 293 K. Therefore, the experimental results strongly confirmed our predictions, and moreover, such reactivity is also helpful to understand the impressionable electron spin of anion radicals discussed above.

In summary, Y_2@C_{82}-C_s, Y_2C_2@C_{82}-C_s, and Sc_2C_2@C_{82}-C_s were prepared, and the comparative studies on their anion radicals were investigated. On the basis of the ESR spectroscopy and theoretical calculations, it is revealed that the electron spin of metallofullerenes can be manipulated by adjusting the encapsulated species inside the same C_{82}-C_s cage. Concretely, a large manipulation is obtained by changing the internal species from Y_2 to Y_2C_2, and a fine manipulation of the spin distribution is further achieved by changing the encapsulated metal from yttrium to scandium.

■ ASSOCIATED CONTENT

Supporting Information

The HPLC data, mass spectra, UV–vis spectra, Raman spectra, CV spectra, and calculation results. This material is available free of charge via the Internet at http://pubs.acs.org.

■ AUTHOR INFORMATION

Corresponding Author

*E-mail: wangtais@iccas.ac.cn (T.W.); crwang@iccas.ac.cn (C.W.).

Notes

The authors declare no competing financial interest.

■ ACKNOWLEDGMENTS

We thank the National Basic Research Program (2012CB932900), National Natural Science Foundation of China (21121063, 21203205, and 21241004), NSAF (11179006), and China Postdoctoral Science Foundation (201104153).

■ REFERENCES

(1) Shinohara, H. Endohedral Metallofullerenes. *Rep. Prog. Phys.* **2000**, *63*, 843–892.

(2) Chaur, M. N.; Melin, F.; Ortiz, A. L.; Echegoyen, L. Chemical, Electrochemical, and Structural Properties of Endohedral Metallofullerenes. *Angew. Chem., Int. Ed.* **2009**, *48*, 7514–7538.

(3) Yang, S. F.; Liu, F.; Chen, C.; Jiao, M.; Wei, T. Fullerenes Encaging Metal Clusters-Clusterfullerenes. *Chem. Commun.* **2011**, *47*, 11822–11839.

(4) Lu, X.; Feng, L.; Akasaka, T.; Nagase, S. Current Status and Future Developments of Endohedral Metallofullerenes. *Chem. Soc. Rev.* **2012**, *41*, 7723–7760.

(5) Yamada, M.; Akasaka, T.; Nagase, S. Endohedral Metal Atoms in Pristine and Functionalized Fullerene Cages. *Acc. Chem. Res.* **2010**, *43*, 92–102.

(6) Lu, X.; Akasaka, T.; Nagase, S. Chemistry of Endohedral Metallofullerenes: The Role of Metals. *Chem. Commun.* **2011**, *47*, 5942–5957.

(7) Popov, A. A.; Dunsch, L. Electrochemistry In Cavea: Endohedral Redox Reactions of Encaged Species in Fullerenes. *J. Phys. Chem. Lett.* **2011**, *2*, 786–794.

(8) Meyer, C.; Harneit, W.; Naydenov, B.; Lips, K.; Weidinger, A. N@C_{60} and P@C_{60} as Quantum Bits. *Appl. Magn. Reson.* **2004**, *27*, 123–132.

(9) Farrington, B. J.; Jevric, M.; Rance, G. A.; Ardavan, A.; Khlobystov, A. N.; Briggs, G. A. D.; Porfyrakis, K. Chemistry at the Nanoscale: Synthesis of an N@C_{60}–N@C_{60} Endohedral Fullerene Dimer. *Angew. Chem., Int. Ed.* **2012**, *51*, 3587–3590.

(10) Liu, G. Q.; Khlobystov, A. N.; Charalambidis, G.; Coutsolelos, A. G.; Briggs, G. A. D.; Porfyrakis, K. N@C_{60}–Porphyrin: A Dyad of Two Radical Centers. *J. Am. Chem. Soc.* **2012**, *134*, 1938–1941.

(11) Aromi, G.; Aguila, D.; Gamez, P.; Luis, F.; Roubeau, O. Design of Magnetic Coordination Complexes for Quantum Computing. *Chem. Soc. Rev.* **2012**, *41*, 537–546.

(12) Yamada, M.; Nakahodo, T.; Wakahara, T.; Tsuchiya, T.; Maeda, Y.; Akasaka, T.; Kako, M.; Yoza, K.; Horn, E.; Mizorogi, N.; Kobayashi, K.; Nagase, S. Positional Control of Encapsulated Atoms Inside a Fullerene Cage by Exohedral Addition. *J. Am. Chem. Soc.* **2005**, *127*, 14570–14571.

(13) Inoue, T.; Tomiyama, T.; Sugai, T.; Okazaki, T.; Suematsu, T.; Fujii, N.; Utsumi, H.; Nojima, K.; Shinohara, H. Trapping a C_2 Radical in Endohedral Metallofullerenes: Synthesis and Structures of (Y_2C_2)@C_{82} (Isomers I, II, and III). *J. Phys. Chem. B* **2004**, *108*, 7573–7579.

(14) Olmstead, M. M.; de Bettencourt-Dias, A.; Stevenson, S.; Dorn, H. C.; Balch, A. L. Crystallographic Characterization of the Structure of the Endohedral Fullerene {$Er_2@C_{82}$ Isomer I} with C_s Cage Symmetry and Multiple Sites for Erbium along a Band of Ten Contiguous Hexagons. *J. Am. Chem. Soc.* **2002**, *124*, 4172−4173.
(15) Lu, X.; Nakajima, K.; Iiduka, Y.; Nikawa, H.; Mizorogi, N.; Slanina, Z.; Tsuchiya, T.; Nagase, S.; Akasaka, T. Structural Elucidation and Regioselective Functionalization of An Unexplored Carbide Cluster Metallofullerene $Sc_2C_2@C_s(6)$-C_{82}. *J. Am. Chem. Soc.* **2011**, *133*, 19553−19558.
(16) Jakes, P.; Dinse, K. P. Chemically Induced Spin Transfer to an Encased Molecular Cluster: An EPR Study of $Sc_3N@C_{80}$ Radical Anions. *J. Am. Chem. Soc.* **2001**, *123*, 8854−8855.
(17) Zuo, T. M.; Xu, L. S.; Beavers, C. M.; Olmstead, M. M.; Fu, W. J.; Crawford, D.; Balch, A. L.; Dorn, H. C. $M_2@C_{79}N$ (M = Y, Tb): Isolation and Characterization of Stable Endohedral Metallofullerenes Exhibiting M−M Bonding Interactions Inside Aza[80]fullerene Cages. *J. Am. Chem. Soc.* **2008**, *130*, 12992−12997.
(18) Popov, A. A.; Chen, N.; Pinzon, J. R.; Stevenson, S.; Echegoyen, L.; Dunsch, L. Redox-Active Scandium Oxide Cluster inside a Fullerene Cage: Spectroscopic, Voltammetric, Electron Spin Resonance Spectroelectrochemical, and Extended Density Functional Theory Study of $Sc_4O_2@C_{80}$ and Its Ion Radicals. *J. Am. Chem. Soc.* **2012**, *134*, 19607−19618.
(19) Delley, B. An All-Electron Numerical-Method for Solving the Local Density Functional for Polyatomic-Molecules. *J. Chem. Phys.* **1990**, *92*, 508−517.
(20) Perdew, J. P.; Burke, K.; Ernzerhof, M. Generalized Gradient Approximation Made Simple. *Phys. Rev. Lett.* **1996**, *77*, 3865−3868.
(21) Bingel, C. Cyclopropylation of Fullerenes. *Chem. Ber.* **1993**, *126*, 1957−1959.

dx.doi.org/10.1021/jz3020666 | *J. Phys. Chem. Lett.* 2013, 4, 464−467